Transverse load redistribution and effective shear width in reinforced concrete slabs

E.O.L. Lantsoght [1,2], C. van der Veen [1], A. de Boer [3], J.C. Walraven [1]

[1] Delft University of Technology, the Netherlands

[2] Universidad San Francisco de Quito, Ecuador

[3] Ministry of Infrastructure and the Environment, the Netherlands

In slabs subjected to concentrated loads close to the support, shear is verified for two limit states: beam shear over an effective width, and punching shear on a perimeter around the concentrated load. In current practice, the beam shear strength of slabs is calculated as for beams, and thus the beneficial effects of transverse load redistribution in slabs are not considered. An experimental program was conducted at Delft University of Technology to determine the shear capacity of slabs under concentrated loads close to the support. This paper presents the results of the tests conducted on continuous slabs and slab strips. The influence of the loading sequence, size of the loaded area, moment distribution at the support and distance between the load and the support is studied and discussed with regard to the behaviour in slabs and slab strips. It is recommended to use the effective width based on a load spreading method as used in French practice. This recommendation is based on the experimental results, a statistical analysis and non-linear finite element models. The parameter analyses show an increased capacity in slabs as compared to beams as the result of transverse load distribution. The shear capacity of slabs under concentrated loads close to supports can be calculated based on the Eurocode provisions for shear over the recommended effective width.

Key words: Effective width, load redistribution, punching, reinforced concrete, slabs, shear

1 Introduction

The problem of determining the shear capacity of a slab under a concentrated load close to the support occurs when the concentrated loads of live load models are applied to, for example, slab bridges. The incentive for the research on the shear capacity of slabs under

concentrated loads came from analysing existing slab bridges. With the implementation of the Eurocodes, the shear provisions have become more conservative in EN 1992-1-1:2005 (CEN [2005]) as compared to NEN 6720:1995 (Code Committee 351001 [1995]) and the prescribed live loads in EN 1991-2:2003 (CEN [2003]) are heavier and with a smaller axle distance. A number of existing reinforced concrete slab bridges designed according to the previous Dutch national codes was found to be shear-critical upon assessment. Therefore, a further study of shear in slabs under a concentrated load close to the support was necessary (Lantsoght, et al. [2012a]).

Shear in reinforced concrete one-way slabs loaded with a concentrated load close to the support is typically checked in two ways: by calculating the beam shear capacity over a certain effective width, as not the whole width can be activated to carry the shear force, and by checking the punching shear capacity on a perimeter around the load. The beam shear capacity as prescribed by the codes is the result of a statistical analysis of experimental shear capacities from small, heavily-reinforced, simply-supported beams in a four-point bending test. The empirical expression for the shear capacity from EN 1992-1-1:2005 was derived by Regan [1987]. The method of horizontal load spreading, resulting in the effective width b_{eff} of the support which carries the load, depends on local practice. In most cases (e. g. Dutch practice) horizontal load spreading is assumed under a 45° angle from the centre of the load towards the support, Figure 1a. In French practice (Chauvel, et al. [2007]), load spreading is assumed under a 45° angle from the far corners of the loaded area towards the support, Figure 1b. The *fib* Model Code 2010 [2012] provides recommendations for the effective width based on another load spreading method, as shown in Figure 1c. Other methods for the effective width are found in the literature, in which the effective width is determined based on a formula. Lubell, Bentz and Collins [2008] define a reduction factor β_L on the slab width b so that the effective width is $\beta_L b$:

$$\beta_L = 0.7 + 0.3\kappa$$
$$\kappa = \min\left(\frac{b_{\text{load}}}{b}; \frac{b_{\text{sup}}}{b}\right) \quad (1)$$

with:

b the member width;

b_{load} the width of the load;

b_{sup} the width of the support.

Grasser and Thielen [1991] defined the effective width that is used in German practice for simply supported one-way slabs as:

$$b_{eff} = t_y + 0.5x \le b$$
$$t_y = b_{\text{load}} + d_l \tag{2}$$

In Equation (2), x is the centre-to-centre distance between the load and the support and d_l the effective depth to the longitudinal reinforcement. The expression is valid provided that $0 < x < l$, $t_y \le 0.8\,l$ and $t_x \le l$ with $t_x = l_{\text{load}} + d$. The values of t_x and t_y are the size of the wheel print, distributed to mid-depth of the concrete slab, and l is the span length. For loads at a clamped end, $b_{eff} = t_y + 0.3\,x$, valid for $0.2 < x < l$, $t_y \le 0.4\,l$ and $t_x \le 0.2\,l$. For bridge decks, Zheng et al. [2010] defined the effective width as follows (with l_{load} the loaded length):

$$b_{eff} = l_{\text{load}} + l\,(1 - r_{cp})\tan\Phi$$
$$r_{cp} = \frac{b_{\text{load}}}{l} \le 0.4 \tag{3}$$
$$\Phi = 23.3\,r_{cp} + 35.1$$

In Equation (3), the value of Φ is given in degrees. A last method for finding the effective width is from the Swedish Code BBK 79:

$$b_{eff} = \max(b_{\text{load}} + 7d_l;\ 0.65(b_{\text{load}} + l_{\text{load}}) + 10.65d_l) \tag{4}$$

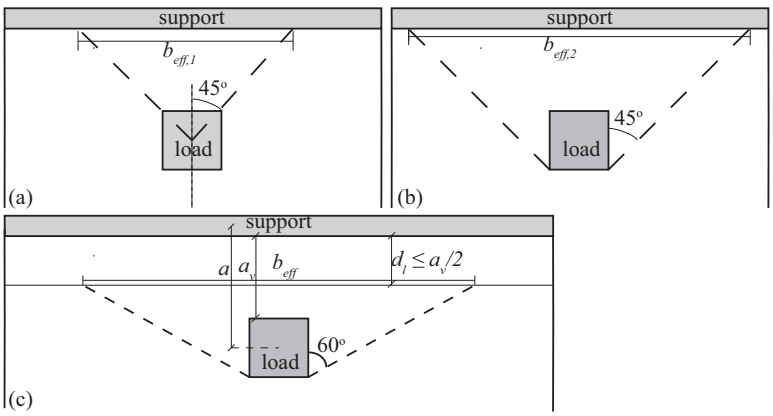

Figure 1. Effective width (a) assuming 45° load spreading from the centre of the load: $b_{eff\,1}$; (b) assuming 45° load spreading from the far corners of the load: $b_{eff\,2}$; top view of slab; (c) load spreading method from fib Model Code 2010 [2012]

The punching shear (two-way shear) capacity in code formulas is developed for two-way slabs. Most empirical methods for punching shear have been derived from tests on slab-column connections; a loading situation which is significantly different from a slab under a concentrated load close to the support.

2 Previous experiments from literature

Recent research as carried out by Sherwood, et al. [2006] concerning shear in slabs focused on one-way slabs under line loads. It was experimentally shown that one-way slabs under line loads behave like beams and that beam shear provisions lead to good estimates of their shear capacity.

A database of 215 experiments on wide beams and slabs (Lantsoght [2012a]) shows that test data regarding the shear capacity of one-way slabs and slab strips under concentrated loads are scarce. In total, 36 experiments with $a/d_l < 2.5$ are available in the literature, Table 1. In Table 1, the following symbols are used:

- b total width of the specimen;
- a the shear span: the centre-to-centre distance between the load and the support;
- d_l the effective depth to the longitudinal flexural reinforcement;
- b_{load} the width of the loaded area, taken parallel to the span direction;
- l_{load} the length of the loaded area, taken perpendicular to the span direction;
- $f_{c,cyl}$ the average cylinder compressive strength of the specimen;
- P_u the ultimate load.
- FM the failure mode, as observed from the available photographs or crack pattern drawings in the cited reference;
- P punching shear failure, development of a (partial) punching cone at the bottom of the slab is visible;
- WB wide beam shear failure: shear failure at the side face, and/or inclined cracks on the bottom face of the slab.

The criterion for activating the transverse load redistribution is that the effective width based on the French load spreading method $b_{eff\,2}$ from Figure 1b is smaller than the total specimen width b. Only 22 of the 215 experiments of a wide beams and slabs database fulfil this requirement, in addition to loading with a concentrated load close to the support.

Table 1. Overview of test data of slabs in shear under concentrated loads close to the support ($a/d_l \leq 2.5$)

Reference	Nr.	b (m)	a/d_l	$b_{load} \times l_{load}$ (mm × mm)	$f_{c,cyl}$ (MPa)	P_u (kN)	FM
Regan [1982]	2SS	1.2	2.16	100 × 100	23.0	130	P
	2CS	1.2	2.16	100 × 100	23.0	180	P
	3SS	1.2	1.68	100 × 100	30.1	195	P
	3CS	1.2	1.68	100 × 100	30.1	250	WB
	4SS	1.2	1.44	100 × 100	35.1	230	P
	5SS	1.2	2.16	200 × 100	30.3	190	P
	7SS	1.2	1.68	200 × 100	36.7	200	P
	7CS	1.2	2.16	200 × 100	36.7	230	P
Furuuchi, et al. [1998]	A-10-10	0.5	1.75	100 × 50	26.1	294	P/WB
	A-10-20	0.5	1.75	100 × 50	20.2	294	WB
	A-10-30	0.5	1.75	100 × 50	23.8	333	WB
	A-20-10	0.5	1.75	200 × 50	19.6	340	-
	A-30-10	0.5	1.75	300 × 50	23.8	450	-
	B-10-10	0.65	1.75	100 × 50	29.4	368	-
	C-10-10	0.5	1.25	100 × 50	34.6	480	WB
	C-20-10	0.5	1.25	200 × 50	32.1	525	WB
	C-30-10	0.5	1.25	300 × 50	31.5	626	WB
	C-50-10	0.5	1.25	500 × 50	34.9	811	WB
	C-10-20	0.5	1.25	100 × 50	36.4	483	-
	C-10-30	0.5	1.25	100 × 50	30.7	520	-
	D-10-10	0.5	2.25	100 × 50	35.2	294	-
Graf [1933]	1243 a_1	2	1.30	100 × 150	19.1	314	WB
	1243 a_2	2	2.17	100 × 150	19.1	235	P/WB
	1243 b_1	2	0.65	100 × 150	19.1	355	P
	1243 b_2	2	1.52	100 × 150	19.1	206	WB
	1244 a_1	2	1.92	100 × 150	13.3	275	WB
	1244 a_2	2	2.40	100 × 150	13.3	196	WB
	1244 b_1	2	1.68	100 × 150	13.3	157	WB
	1244 b_2	2	2.16	100 × 150	13.3	147	WB
	1245 a_1	2.4	1.89	100 × 150	23.6	333	P/WB
	1245 a_2	2.4	2.36	100 × 150	23.6	257	WB
	1245 b_1	2.4	1.65	100 × 150	23.6	196	P/WB
	1245 b_2	2.4	2.12	100 × 150	23.6	206	P/WB
Richart and Kluge [1939]	2-2	6.1	1.64	150‡	29.1	369	P/WB
Leonhardt and Walther [1962]	P12	0.5	2.46	80 × 80	12.6	101†	WB
Ekeberg, et al. [1982]	2nd fl nr. 3	5	2.18	100 × 100	17.8	465	-

-: Photographs or a description of the failure mode were not provided.

†: self-weight is reported to be included in the value of the ultimate load.

‡: a disc is used as loading plate, the diameter is given.

The majority of these experiments were carried out on small specimens (d_l < 15cm). These experiments have been compared to the governing design codes. The results (Lantsoght [2012b]) indicate that slabs can support higher concentrated loads than beams as a result of their extra dimension. However, not enough experimental evidence is available to support this statement. Therefore, a series of experiments on slabs with d_l = 265 mm was carried out.

3 Experiments

3.1 ***Setup***

To study the shear capacity of slabs under a concentrated load close to the support, experiments are carried out. A top view of the test setup with a slab is presented in Figure 2. The line supports used for S1 – S14 and the slab strips are composed of a steel beam (HEM 300) of 300 mm wide, a layer of plywood and a layer of felt of 100 mm wide. The properties of the plywood and felt are described by Prochazkova and Lantsoght [2011]. In S15 – S18, 3 elastomeric bearings of 350 mm × 280 mm × 45 mm are used per side as a support. Over the depth, the bearings contain 3 layers of 8 mm natural rubber, 4 layers of 4 mm steel S235 and 2 layers of 2.5 mm chloroprene, resulting in a compressive stiffness of 2361 kN/mm.

Experiments are carried out close to the simple support (sup 1 in Figure 2) and close to the continuous support (sup 2 in Figure 2). The rotation at support 2 is partly restrained by vertical prestressing bars that are fixed to the strong floor of the laboratory. This restraint results in a moment over support 2: the continuous support. The prestressing force is applied on the bars before the start of every test. During the course of the experiment, some rotation could occur over support 2 due to the deformation of the felt and plywood and the elongation of the prestressing bars. The force in the prestressing bars is measured throughout the experiments by means of load cells.

3.2 ***Specimens***

An overview of the specimens that are tested in the first series of experiments is given in Table 2, using the following symbols and abbreviations:

b the width of the specimen;

$f_{c,\text{cube}}$ the measured cube compressive strength of the concrete at the age of testing;

$f_{ct,\text{cube}}$ the measured cube splitting strength of the concrete at the age of testing;

ρ_l	the longitudinal flexural reinforcement ratio;
ρ_t	the transverse flexural reinforcement ratio;
a	the shear span: the centre-to-centre distance between the load and the support;
d_l	the effective depth to the longitudinal reinforcement;
n	the number of experiments on the considered specimen;
M/E	the concentrated load is placed in the middle of the width (M) or near the edge (E) for the uncracked experiments;
z_{load}	the size of side of the square loaded area;
age	the age at which the specimen is tested for the first time.

All slabs and slab strips had a height of 300 mm. The effective depth to the longitudinal flexural reinforcement is d_l = 265 mm for S1 – S14 and the slab strips, and is d_l = 255 mm for S15 – S18 (slabs supported by bearings).

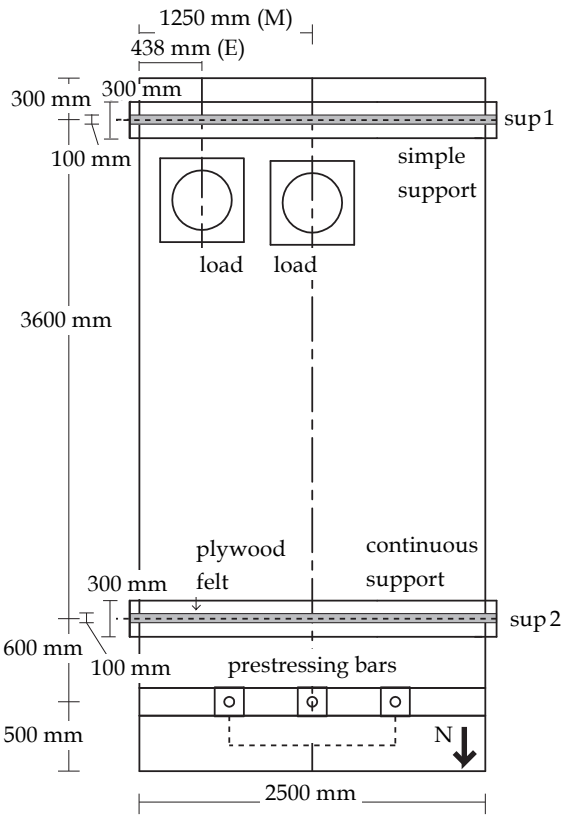

Figure 2. Sketch of test setup for S1 – S14, top view

The numbering for the slabs starts with "S", while for the slab strips or beams ("B") the numbering is subdivided according to the width: S (b = 0.5 m), M (b = 1 m), L (b = 1.5 m) or X (b = 2 m). The slabs were either loaded at the middle of the slab width (position M) at the simple and continuous support, resulting in two tests per slab that are "uncracked" (one at the simple support and one at the continuous support) and maximum four tests that are considered "cracked", see Figure 3. These "cracked" experiments were executed after the first, "uncracked" experiments, so that the cracks and failure of the "uncracked" experiments influenced the capacity of the "cracked" experiment. Executing an experiment in the vicinity of a the failure cracks from an earlier experiment can give a lower bound estimate of the shear capacity of bridge slabs that are fully cracked in bending after being in service for several decades.

Table 2. Properties of S1 – S18 and the series of slab strips

Slab nr.	b (m)	$f_{c,\mathrm{cube}}$ (MPa)	$f_{ct,\mathrm{meas}}$ (MPa)	ρ_l (%)	ρ_t (%)	a/d_l	n	M/E	z_{load} (mm)	age
S1	2.5	35.8	3.1	0.996	0.132	2.26	6	M	200	28
S2	2.5	34.5	2.9	0.996	0.132	2.26	6	M	300	56
S3	2.5	51.6	4.1	0.996	0.258	2.26	5	M	300	63
S4	2.5	50.5	4.1	0.996	0.182	2.26	6	E	300	76
S5	2.5	46.2	3.6	0.996	0.258	1.51	5	M	300	31
S6	2.5	58.2	3.9	0.996	0.258	1.51	6	E	300	41
S7	2.5	82.1	6.2	0.996	0.258	2.26	6	E	300	83
S8	2.5	77.0	6.0	0.996	0.258	2.26	3	M	300	48
S9	2.5	81.7	5.8	0.996	0.258	1.51	6	M	200	77
S10	2.5	81.6	5.8	0.996	0.258	1.51	7	E	200	90
S11	2.5	54.9	4.2	1.375	0.358	2.26	6	M	200	90
S12	2.5	54.8	4.2	1.375	0.358	2.26	6	E	200	97
S13	2.5	51.9	4.2	1.375	0.358	1.51	6	M	200	91
S14	2.5	51.3	4.2	1.375	0.358	1.51	6	E	200	110
S15	2.5	52.2	4.2	1.035	1.078	2.35	5	M	200	71
S16	2.5	53.5	4.4	1.035	1.078	2.35	6	E	200	85
S17	2.5	49.4	3.7	1.035	1.078	1.57	6	M	200	69
S18	2.5	52.1	4.5	1.035	1.078	1.57	6	E	200	118
BS1	0.5	81.5	6.1	0.948	0.258	2.26	2	M	300	55
BM1	1	81.5	6.1	0.948	0.258	2.26	2	M	300	62
BL1	1.5	81.5	6.1	0.948	0.258	2.26	2	M	300	189
BS2	0.5	88.6	5.9	0.948	0.258	1.51	2	M	200	188
BM2	1	88.6	5.9	0.948	0.258	1.51	2	M	200	188
BL2	1.5	94.8	5.9	0.948	0.258	1.51	2	M	200	180
BS3	0.5	91.0	6.2	0.948	0.258	2.26	2	M	300	182
BM3	1	91.0	6.2	0.948	0.258	2.26	2	M	300	182
BL3	1.5	81.4	6.2	0.948	0.258	2.26	2	M	300	171
BX1	2	81.4	6.0	0.948	0.258	2.26	2	M	300	47
BX2	2	70.4	5.8	0.948	0.258	1.51	2	M	200	39
BX3	2	78.8	6.0	0.948	0.258	2.26	2	M	200	40

Alternatively, the slabs were loaded consecutively at the east and west side (position E) at the simple and continuous support, resulting in four "uncracked" tests per slab and maximum two "cracked" tests. The experiments are numbered as SxTy with x the specimen number and y the number of the test on this specimen. These test numbers are taken consecutively and do not denote the location of the load (position M or E), see §4.1.

Deformed bars of steel S500 (measured properties for ø20 mm: f_{ym} = 542 MPa yield strength; f_{um} = 658 MPa ultimate strength and for ø10 mm: f_{ym} = 537 MPa; f_{um} = 628 MPa) were used. Plain bars of steel 52.3K (measured properties for ø20 mm: f_{ym} = 601 MPa; f_{um} = 647 MPa and for ø10 mm: f_{ym} = 635 MPa; f_{um} = 700 MPa) were used. The flexural reinforcement was designed to resist a moment caused by a load of 2 MN (maximum capacity of the jack) at position M along the width (Figure 2) and at 600 mm along the span (a/d_l = 2.26).

According to EN 1992-1-1:2005 §9.3.1.1(2), the amount of transverse flexural reinforcement for slabs needs to be taken as 20% of the longitudinal flexural reinforcement. In the tested slabs, 13.3% of the longitudinal flexural reinforcement was used as transverse reinforcement in S1 and S2; 25.9% in S3, S5-S10 and the slab strips; 26.0% in S11-S14 (different reinforcement layout for slabs with plain bars); and 104% in S15 – S18, where a virtual beam of heavy reinforcement above the support is used for the slabs supported by

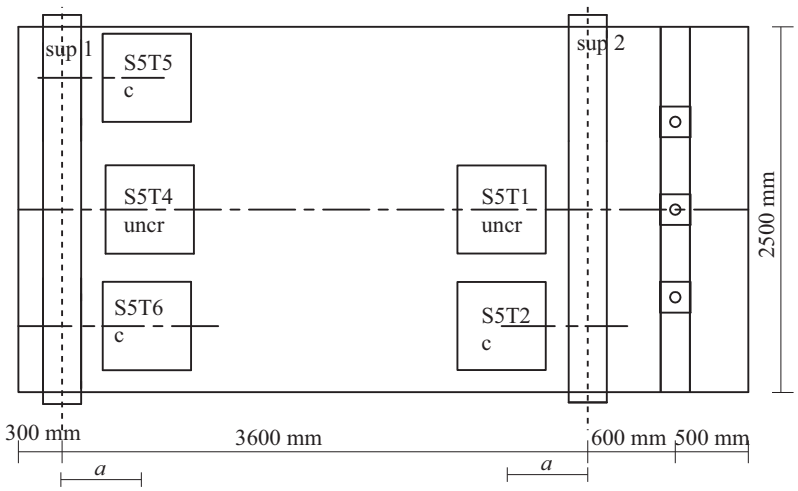

Figure 3. Loading sequence on a slab, taking S5 as an example

bearings (instead of a line support). In S4 the amount of transverse flexural reinforcement is only doubled as compared to S1 and S2 in the vicinity of the supports. Figure 4 shows elevation, cross-section and detailing of the reinforcement in S1 – S10, Figure 5 shows the reinforcement layout of the slabs with plain bars (S11 - S14) and the slabs supported by bearings (S15 – S18). Figure 6 shows the reinforcement layout as used for the slab strips demonstrated for BS1-BS3. Similar reinforcement is used in the BM, BL and BX-series, with the number of bars proportionally increased with the increasing width.

Two types of concrete have been used: normal strength concrete (C28/35) for slabs S1 – S6 and S11 – S18 and high strength concrete (C55/65) for slabs S7 – S10 and the slab strips. Glacial river aggregates with a maximum aggregate size of 16 mm were used.

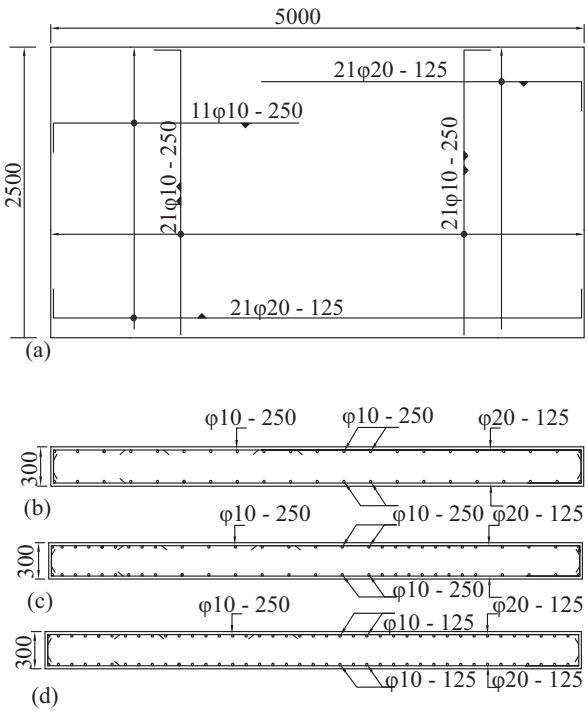

Figure 4. Reinforcement layout of slabs with line supports: (a) plan view of S1 and S2, (b) section of S1 and S2, (c) section of S4, (d) section of S3, S5-S10, in [mm]

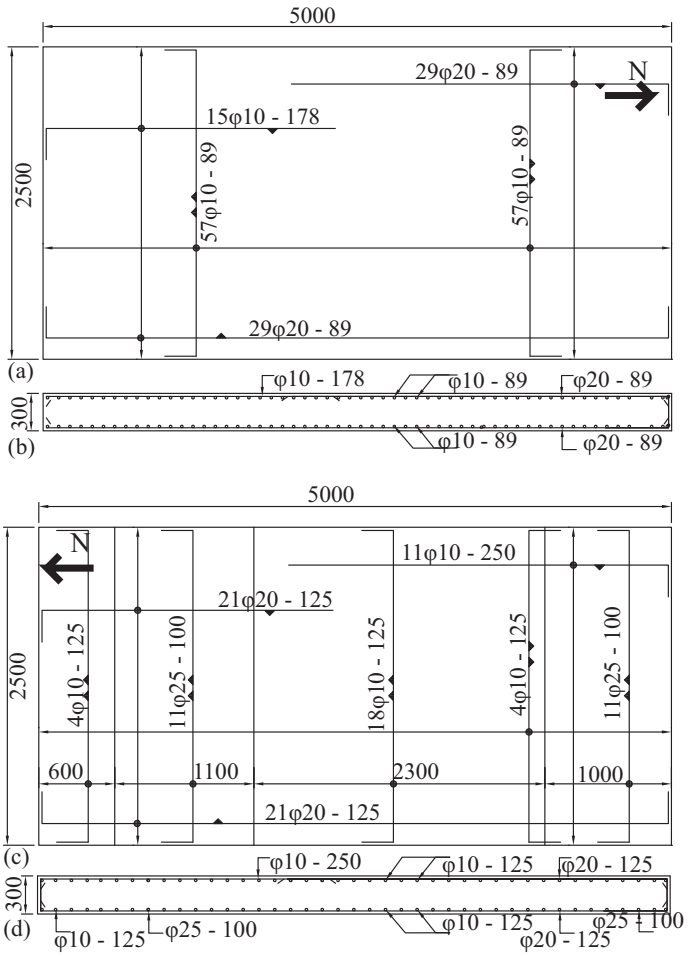

Figure 5. Reinforcement layout for slabs with plain reinforcement or supported by elastomeric bearings: (a) top view of S11-S14; (b) cross section of S11-S14; (c) top view of S15-S18; (d) cross section of S15-S18 in [mm]

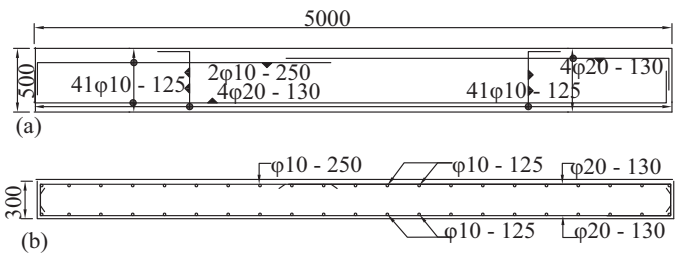

Figure 6. Reinforcement layout for slab strips: (a) top view of BS1; (b) cross section of BS1 in [mm]

4 Results

4.1 *Test Results*

The number of the specimen is followed by the number of the test on this specimen (e. g. S6T2: 2nd test on 6th slab). The experimental results of the slabs and slab strips are summarized in Table 3, in which the following symbols are used:

a/d_l	the ratio of the distance between the load and the support (or shear span) to the effective depth to the longitudinal reinforcement;
b_r	the distance between the centre of the loaded area and the free edge of the slab along the width;
SS/CS	the position of the load: close to the simple support (SS) or the continuous support (CS);
uncr/c	experiment on an uncracked specimen (uncr) or on a previously tested, locally failed and severely damaged specimen (c);

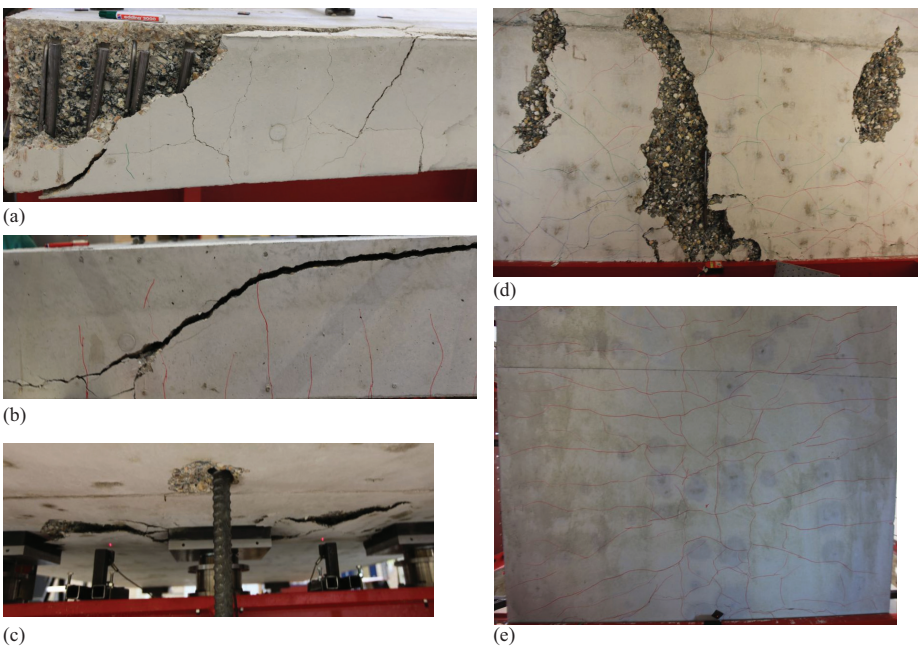

Figure 7. (a) A: Anchorage failure (S11T3); (b) B: shear crack at the side face (BL3T1); (c) SF: failure at the support (S17T1); (d) P: partial punching at the bottom face (S14T6); (e) WB crack pattern: inclined cracks on the bottom face (BL3T1)

P_u the measured ultimate load at the concentrated load during the experiment;

F_{pres} the sum of the forces in the 3 prestressing bars;

V_{exp} the shear force at the support as a result of the self-weight of the slab, the concentrated load and the force in the prestressing bars;

Observed failure mode:

- anchorage failure (A, Figure 7a);
- failure as a beam in shear with a noticeable shear crack at the side (B, Figure 7b);
- punching failure around the support (SF, Figure 7c)
- development of a partial punching surface on the bottom face (P, Figure 7d); or
- failure as a wide beam in shear with inclined cracks on the bottom of the specimen (WB, Figure 7e).

Most slabs were tested within 1 to 2 weeks after the first experiment on the specimen as given in Table 2. A complete description of the experiments on the undamaged specimens can be found in the full test reports by Lantsoght [2011b] and of the residual capacity in the full test report by Lantsoght [2011a].

Table 3. Results from experiments on S1 – S18 and the slab strips

Test	a/d	b_r (mm)	SS/CS	uncr/c	P_u (kN)	Mode	F_{pres} (kN)	V_{exp} (kN)
S1T1	2.26	1250	SS	uncr	954	WB	163	799
S1T2	2.26	1250	CS	uncr	1023	WB	138	912
S1T3	2.34	438	CS	c	758	WB + B	87	683
S1T4	2.26	438	CS	c	731	WB + B	100	663
S1T5	2.26	438	SS	c	851	WB + B	147	716
S1T6	2.26	438	SS	c	659	WB + B	145	556
S2T1	2.26	1250	SS	uncr	1374	WB + P	280	1129
S2T2	2.26	438	SS	c	1011	WB + B	228	835
S2T3	2.26	438	SS	c	844	WB + B	248	693
S2T4	2.26	1250	CS	uncr	1421	WB	330	1276
S2T5	2.26	438	CS	c	805	WB + B	153	733
S2T6	2.26	438	CS	c	957	WB + B	177	864
S3T1	2.26	1250	SS	uncr	1371	WB	252	1131
S3T2	2.26	438	SS	c	993	WB + B	245	818
S3T3	2.26	438	SS	c	705	WB + B	190	587
S3T4	2.26	1250	CS	uncr	1337	WB + B	287	1199

S3T5	2.26	438	CS	c	852	WB + B	128	768
S4T1	2.26	438	SS	uncr	1160	WB + B	203	964
S4T2	2.26	438	SS	uncr	1110	WB + B	187	925
S4T3	2.26	1250	SS	c	1016	WB	227	840
S4T4	2.26	438	CS	c	861	WB + B	158	781
S4T5	2.26	438	CS	c	1014	WB + B	185	913
S4T6	2.26	1250	CS	c	994	WB	147	889
S5T1	1.51	1250	CS	uncr	1804	WB + B	235	1679
S5T2	1.51	438	CS	c	1395	WB + B	162	1304
S5T4	1.51	1250	SS	uncr	1755	WB + B	280	1544
S5T5	1.51	438	SS	c	1295	WB + B	227	1144
S5T6	1.51	438	SS	c	1286	WB + B	170	1146
S6T1	1.51	438	CS	uncr	1446	WB + B	183	1353
S6T2	1.51	438	CS	uncr	1423	WB + B	213	1337
S6T3	1.51	1250	CS	c	1897	WB	313	1775
S6T4	1.51	438	SS	uncr	1366	WB + B	195	1213
S6T5	1.51	438	SS	uncr	1347	WB + B	245	1187
S6T6	1.51	1250	SS	c	1384	WB	270	1216
S7T1	2.26	438	SS	uncr	1121	WB + P + B	217	929
S7T2	2.26	438	CS	uncr	1172	WB + P + B	197	1046
S7T3	2.26	438	CS	uncr	1136	WB + P + B	227	1021
S7T4	2.26	1250	CS	c	1128	WB + P	188	1008
S7T5	2.26	438	SS	uncr	1063	WB + P + B	157	891
S7T6	2.26	1250	SS	c	1011	WB + P	443	799
S8T1	2.26	1250	SS	uncr	1481	WB + B	233	1226
S8T2	2.26	1250	CS	uncr	1356	WB + B	278	1213
S8T5	2.26	438	SS	c	868	WB + B	160	728
S9T1	1.51	1250	SS	uncr	1523	WB + P	175	1355
S9T2	1.51	438	SS	c	929	WB + P + B	142	833
S9T3	1.51	438	SS	c	1089	WB + P + B	178	969
S9T4	1.51	1250	CS	uncr	1842	WB + P	255	1717
S9T5	1.51	438	CS	c	1287	WB + B	138	1204
S9T6	1.51	438	CS	c	1128	WB + B	87	1054
S10T1	1.51	438	SS	uncr	1320	WB + P + B	162	1177
S10T2	1.51	438	SS	uncr	1116	WB + P + B	173	994
S10T3	1.51	1250	SS	c	1326	WB + P	320	1156
S10T4	1.51	438	CS	uncr	1511	WB + (B)	252	1422
S10T4B	1.51	438	CS	c	1058	WB + B	165	1005
S10T5	1.51	438	CS	uncr	1454	WB + B	235	1368
S10T6	1.51	1250	CS	c	1431	WB	233	1348

S11T1	2.26	1250	SS	uncr	1194	WB + P	165	998
S11T2	2.26	438	SS	c	869	P	162	728
S11T3	2.26	438	SS	c	890	WB + P + B + A	253	730
S11T4	2.26	1250	CS	uncr	958	WB + P	307	886
S11T5	2.26	438	CS	c	566	WB + B	180	538
S11T6	2.26	438	CS	c	492	WB + B	147	471
S12T1	2.26	438	SS	uncr	931	WB + B + P	162	780
S12T2	2.26	438	SS	uncr	1004	P	173	839
S12T3	2.26	1250	SS	c	1053	WB + P	193	876
S12T4	2.26	438	CS	uncr	773	WB + P + B	147	705
S12T5	2.26	438	CS	uncr	806	WB + B	158	735
S12T6	2.26	1250	CS	c	683	WB + P	107	624
S13T1	1.51	1250	SS	uncr	1404	WB + P	157	1253
S13T2	1.51	438	SS	c	1253	WB + P + B	137	1122
S13T3	1.51	438	SS	c	916	WB + P + B	183	815
S13T4	1.51	1250	CS	uncr	1501	WB + P	240	1411
S13T5	1.51	438	CS	c	1062	WB + B	150	1006
S13T6	1.51	438	CS	c	1023	WB + B	150	971
S14T1	1.51	438	SS	uncr	1214	WB + P + B	133	1088
S14T2	1.51	438	SS	uncr	1093	WB + P + B	162	975
S14T3	1.51	1250	SS	c	1385	WB + B	230	1224
S14T4	1.51	438	CS	uncr	1282	WB + P + B	187	1207
S14T5	1.51	438	CS	uncr	1234	WB + P + B	142	1157
S14T6	1.51	1250	CS	c	1304	WB + B	145	1220
S15T1	2.35	1250	CS	uncr	1040	WB + B + SF	245	944
S15T2	2.35	438	CS	c	555	WB + B + SF	102	516
S15T4	2.35	1250	SS	uncr	1127	WB + SF	158	944
S15T5	2.35	438	SS	c	863	WB + B + SF	145	726
S15T6	2.35	438	SS	c	804	WB + B	155	675
S16T1	2.35	438	SS	uncr	932	WB + B	188	776
S16T2	2.35	438	SS	uncr	815	WB + B	208	675
S16T3	2.35	1250	SS	c	593	WB + SF	327	471
S16T4	2.35	438	CS	uncr	776	WB + B + SF	235	723
S16T5	2.35	438	CS	uncr	700	WB + B + SF	198	653
S16T6	2.35	1250	CS	c	570	WB + SF	182	542
S17T1	1.57	1250	CS	uncr	1365	WB + SF	208	1285
S17T2	1.57	438	CS	c	715	WB + B + SF	77	685
S17T3	1.57	438	CS	c	812	WB + B + SF	157	785
S17T4	1.57	1250	SS	uncr	1235	WB + SF	118	1109
S17T5	1.57	438	SS	c	847	WB + B + SF	115	765

S17T6	1.57	438	SS	c	875	WB	117	789
S18T1	1.57	438	SS	uncr	1157	WB + B + SF	170	1031
S18T2	1.57	438	SS	uncr	1079	WB + B	213	954
S18T3	1.57	1250	SS	c	967	WB	280	844
S18T4	1.57	438	CS	uncr	1122	WB + B + SF	167	1062
S18T5	1.57	438	CS	uncr	1104	WB + B + SF	190	1050
S18T6	1.57	1250	CS	c	995	WB + P + SF	185	952
BS1T1	2.26	250	SS	uncr	290	B	37	242
BS1T2	2.26	250	CS	uncr	623	B	212	562
BS2T1	1.51	250	SS	uncr	633	B	100	552
BS2T2	1.51	250	CS	uncr	976	B	267	919
BS3T1	2.26	250	SS	uncr	356	B	57	293
BS3T2	2.26	250	CS	uncr	449	B	107	399
BM1T1	2.26	500	CS	uncr	923	WB + B	160	755
BM1T2	2.26	500	SS	uncr	720	WB + B	127	636
BM2T1	1.51	500	SS	uncr	1212	WB + B	167	1062
BM2T2	1.51	500	CS	c	1458	WB + B	262	1354
BM3T1	2.26	500	SS	uncr	735	WB + B	110	607
BM3T2	2.26	500	CS	uncr	895	WB + B	183	791
BL1T1	2.26	750	SS	uncr	1034	WB + B	215	844
BL1T2	2.26	750	CS	uncr	1252	WB + B	320	1119
BL2T1	1.51	750	SS	uncr	1494	WB + B	212	1311
BL2T2	1.51	750	CS	uncr	1708	WB + B	277	1586
BL3T1	2.26	750	SS	uncr	1114	WB + B	242	907
BL3T2	2.26	750	CS	uncr	1153	WB + B	312	1035
BX1T1	2.26	1000	SS	uncr	1331	WB + P	325	1080
BX1T2	2.26	1000	CS	uncr	1596	WB + B + P	335	1415
BX2T1	1.51	1000	SS	uncr	1429	WB + B + P	217	1259
BX2T2	1.51	1000	CS	uncr	1434	WB + P	167	1332
BX3T1	2.26	1000	SS	uncr	1141	WB + P	245	935
BX3T2	2.26	1000	CS	uncr	1193	WB + B	210	1059

*4.2 **Loading Sequence***

Concerning the shear or punching capacity of pre-cracked concrete beams and slabs, very few experiments are available in the literature. For aggregate interlock, an important shear-carrying mechanism, Hofbeck et al. [1969] argument that, if a crack exists in the shear plane before the application of shear, then the slip at all stages of loading will be greater than would have occurred if the crack had not been present. In their push-off experiments, the existence of a crack in the shear plane reduced the ultimate shear strength from

aggregate interlock. Following this argument, Yang [2011] observed similar inclined cracking strengths for pre-cracked beams but lower ultimate strengths, as the pre-cracked beams failed upon or shortly after the formation of the inclined crack. For beams pre-cracked in bending, Hamadi and Regan [1980] did not observe any influence of these cracks on the shear failure. For punching shear, Azad et al. [1993] studied the orientation of the crack in pre-cracked slab-column experiments. For existing cracks under a degree of 20 to 30°, the existing crack had a detrimental effect on the punching shear capacity, which became about 54% of the punching shear capacity of a specimen without an existing crack. For slabs S3 to S18, two specimens were tested with all parameters similar, except the loading sequence (Figure 3). To study the effect of pre-cracking, the result of an experiment on an undamaged specimen is compared to the result of an experiment carried out in the vicinity of a local failure. It was observed that the width of cracks from previous testing increased during testing for residual capacity. S6T3 gave a 5% higher residual capacity than S5T1 and S13T2 gave a 3% higher capacity than S14T2; all other comparisons gave lower residual capacities, as expected. The overall average is a residual capacity of 81% of the undamaged shear strength. This result is surprisingly high, as it was not expected that slabs which had been tested up to their ultimate capacity and showed cracks of sometimes 20 mm to 30 mm wide (Figure 8) would be able to resist considerable loads upon reloading.

The high residual capacity of slabs under concentrated loads close to the support in shear demonstrates the large redistribution capacity of slabs. In the case of an experiment in the vicinity of a local failure, an alternative load carrying path away from the local failure can be found.

*4.3 **Size of the loaded area***

The size of the loaded area is interesting to study, as it does not influence the effective width as determined from the Dutch load spreading method, $b_{eff\,1}$, Figure 1a, while it does

Figure 8. Punching damage at the bottom of a slab after an experiment

influence the effective width as determined from the French load spreading method, $b_{eff\,2}$, Figure 1b.

Test results from the literature that are compared based on the size of the loaded area in Table 4 indicate an increasing shear capacity for an increasing width of the loaded area. The increase in loaded area ("increase load size"), as compared to the loaded area of the experiment on the previous row, and the increase in ultimate capacity ("increase $P_{\exp}$"), as compared to the ultimate capacity of the experiment on the previous row, are shown. Note that the increase in ultimate capacity becomes larger for the largest tested loading plates, while the increase in size of these loading plates is percentage-wise smaller than for the smaller tested loading plates. For smaller a/d_l distances, smaller increases in capacity are reported than for loads applied further away from the support. In these experiments one dimension of the loading plate is constant, leading to an increasing degree of rectangularity. Experiments using square loading plates of different sizes are not available.

Table 4. Increase in ultimate load for an increasing size of the loading plate as reported in literature

Reference	Nr	a/d_l	load (mm × mm)	increase load size	$P_{\exp}$ (kN)	increase $P_{\exp}$
Furuuchi et al. 1998	A-10-10	1.75	100 × 50	-	294	-
	A-20-10	1.75	200 × 50	100%	340	16%
	A-30-10	1.75	300 × 50	50%	450	32%
	C-10-10	1.25	100 × 50	-	480	-
	C-20-10	1.25	200 × 50	100%	525	9%
	C-30-10	1.25	300 × 50	50%	626	19%
	C-50-10	1.25	500 × 50	67%	811	30%
Regan 1982	2SS	2.16	100 × 100	-	130	-
	5SS	2.16	200 × 100	100%	190	46%
	3SS	1.68	100 × 100	-	195	-
	7SS	1.68	200 × 100	100%	200	3%

To study the influence of the size of a square loading plate on the shear capacity of one-way slabs and slab strips, the results of slabs and slabs strips of comparable experiments (in which only the size of the loaded area is changed) are studied. The slabs consist of normal strength concrete and the slab strips of high strength concrete. The results of the comparison of the experimental data are shown in Table 5, displaying the measured average increase in capacity V_u for an increase in size of loading plate from 200 mm × 200 mm to 300 mm × 300 mm. The results of the specimens with widths of 1 m to 2.5 m in Table 5 show that the influence of the loading plate size on the shear capacity becomes larger as the overall specimen size increases (Lantsoght, et al. [2012b]).

Table 5. Measured increase in ultimate shear capacity for an increase in the size of the loaded area from 200 mm × 200 mm to 300 mm × 300 mm

Specimens	b (m)	Average increase V_u
BS1 – BS3	0.5	11.5%
BM1 – BM3	1.0	0.1%
BL1 – BL3	1.5	0.6%
BX1 – BX3	2.0	24.6%
S1 – S2	2.5	40.6%

The influence of the size of the loaded area can be explained based on the transverse load redistribution capacity in slabs. Considering the load distribution as a three-dimensional problem in which compression struts occur over the depth and the width of the slab, it is clear that a larger loaded area provides a larger base for the compressive struts. As these compressive struts develop over a larger area, more material is activated to carry the load and thus the shear capacity is increased.

4.4 Moment distribution at the support

Research from the 60s and 70s indicated a lower shear capacity at the continuous support. Rafla [1971] attributed this observation to the larger rearrangement of the inner forces, the lower quality of bond for the top reinforcement at the support and the combination of larger moments and larger shear forces. As a result, in the former Dutch code NEN 6720:1995, an increase in capacity as a result of direct load transfer can only be accounted for in the case of loads close to the end supports or when no change in the sign of the moment occurs. Regan [1982], however, observed a larger shear capacity at the continuous support, which is expressed by the enhancement factor a_{Regan} .

$$a_{\text{Regan}} = \sqrt{\frac{M_1 + M_2}{M_1}} \tag{5}$$

in which M_1 and M_2 are the larger respectively the smaller moment at either end of the shear span. For Regan's experiments [1982], an average increase in shear capacity at the continuous support of 55% is measured (Table 1), while the calculated increase based on a_{Regan} is 14%. For these results, the correction factor a_{Regan} underestimates the influence of the moment distribution over the support.

All slabs S1 – S18 and slab strips BS1 – BX3 are tested at the simple and continuous support. The execution procedure of the experiments, using prestressing bars that allow

some rotation over the continuous support, is different from those by Regan [1982] in which the rotation at the continuous support was fully restrained.

The experimental results are summarized in Table 6, showing the average (AVG) increase of the shear capacity when an experiment at the continuous support, $V_{exp,CS}$ is compared to an identical experiment at the simple support, $V_{exp,SS}$ and the associated standard deviation (STD) and coefficient of variation (COV). The expected increase based on Regan's proposed factor a_{Regan} is also given. The results show that the shear capacity at the continuous support is larger than the shear capacity at the simple support. The factor a_{Regan} overestimates the effect of the continuous support for all slabs S1 – S18. When studying the results in Table 6 with regard to the specimen width, it is seen that the influence of the moment distribution at the support decreases with an increase in the slab width (Lantsoght [2012c]).

Table 6. Comparison between shear capacity at simple and continuous support

Experiments	b (m)	a_{Regan}	AVG $\frac{V_{exp,CS}}{V_{exp,SS}}$	STD	COV
BS	0.5	1.263	1.783	0.492	28%
BM	1	1.149	1.329	0.069	5%
BL	1.5	1.191	1.225	0.093	8%
BX	2	1.134	1.167	0.130	11%
S1 – S10	2.5	1.150	1.112	0.133	12%
S11 – S14	2.5	1.169	1.015	0.140	14%
S15 – S18	2.5	1.196	1.031	0.085	8%
BS - BX	var	1.184	1.376	0.337	24%

The experimental results indicate that for slabs, the influence of the moment distribution over the support is smaller than for beams. For slabs the transverse moment plays a role for the capacity at the continuous support. It is thus necessary to investigate the combination of longitudinal and transverse moment to assess the influence of the moment distribution at the support. As calculated by Lantsoght [2012c] this observation is reflected by the results of linear finite element calculations, in which the profile of the reaction forces over the support length is studied to determine the theoretical effective width from a linear finite element calculation. The requirement for determining the effective width is theoretically that the reaction resulting from the total shear stress over the full support width should equal the reaction resulting from the maximum shear stress over the effective width. This effective width is smaller at the continuous support as compared to the simple support, indicating the role of the transverse moment. This analysis also shows that

cracking and non-linear behaviour only play a secondary role in the difference between the shear capacity at the simple and the continuous support.

4.5 ***Distance between the load and the support***

In early research by Talbot [1909], Richart [1927] and Clark [1951] it was already known that the distance between the load and the support, expressed as the shear span to depth ratio (a/d_l) is an important parameter influencing the shear capacity.
Kani [1964] showed the influence of the a/d_l ratio on the ratio of maximum moment to theoretical flexural failure moment M_{CR}/M_{FL} and the failure mode, resulting in the so-called valley of shear failure. When the load is placed close to the support, the formation of a concrete compressive strut between the load and the support provides an additional load bearing path after inclined cracking occurs. This mechanism allows for a considerable increase of the load upon the formation of an inclined crack. As a result, decreasing the a/d_l ratio from about 2.5 to 0.5 increases the shear resistance, as a steeper compression strut can carry a larger load.
To take direct load transfer into account, EN 1992-1-1:2005 §6.2.2. (6) allows for the reduction of loads applied within a face-to-face distance a_v between the load and the support between $d_l/2$ and $2d_l$ with a factor $\beta = {a_v}/{2d_l}$. This value is determined by Regan [1998] from beam shear tests and provides a lower bound for the increase in capacity as a_v/d_l decreases.
In the case of slabs under concentrated loads, the influence of the span to depth ratio is not well understood, as two counteracting mechanisms occur: the effective width and the development of the compressive strut. A 45° load spreading in the horizontal direction as shown in Figure 1 leads to a decreasing effective width for a decreasing distance to the support. For a given maximum shear stress v_u , a smaller effective width leads consequently to a smaller maximum theoretical shear capacity V_u , with:

$$V_u = v_u b_{eff} d_l \tag{6}$$

To study the influence of the distance between the load and the support (a/d_l) experimentally, the results of the slabs and slab strips with a = 600 mm and a = 400 mm are compared (Lantsoght, et al. [2013]).

The experimental observations are summarized in Table 7, showing the measured average ratio of the shear capacity for a = 400 mm, $V_{\exp,400}$ to the shear capacity for a = 600 mm,

Table 7. Influence of the decrease in the shear span from 600 mm to 400 mm on the observed increase on the shear capacity

Specimens	b (m)	AVG $\frac{V_{\exp,400}}{V_{\exp,600}}$	standard deviation	coefficient of variation	expected $\frac{V_{\exp,400}}{V_{\exp,600}}$
BS2 – BS3	0.5	2.09	0.297	14.2%	1.8
BM2 – BM3	1	1.73	0.027	1.6%	1.8
BL2 – BL3	1.5	1.49	0.061	4.1%	1.8
BX2 – BX3	2	1.30	0.063	4.8%	1.8
S3 – S6	2.5	1.42	0.172	12.1%	2
S11 – S14	2.5	1.45	0.213	14.7%	1.8
S15 – S18	2.5	1.39	0.145	10.4%	2.25 // 1.41

$V_{\exp,600}$. The results show a clear increase in shear capacity with decreasing distance to the support as well as a clear influence of the overall member width b on the quantity of this increase. The last column of Table 7 shows the expected average ratio of the shear capacity for a = 400 mm as compared to the shear capacity for a = 600 mm based on the factor β from EN 1992-1-1:2005. For S17 and S18 the value of $a_v/2d_l$ = 0.314 which results in β = 0.5. Therefore, the expected increase in capacity is given based on the comparison of a_{v400}/a_{v600} (2.25) and based on β_{400}/β_{600} (1.41). Comparing the expected to the measured increase shows that the observed increase in shear resistance for slabs is less than obtained with the factor β given by EN 1992-1-1:2005 for beam shear.

The observed lower increase and dependence on the width b of the capacity for a decrease in the ratio of distance between the load and the support and the effective depth a/d_l can be explained when studying the compression struts in slabs under concentrated loads. For beams, a clearly defined strut develops over the distance a, while in slabs a fan of struts can develop. A plan view of these struts is shown in Figure 9. This sketch also shows the influence of the width in slabs and the resulting transverse redistribution of the load. In

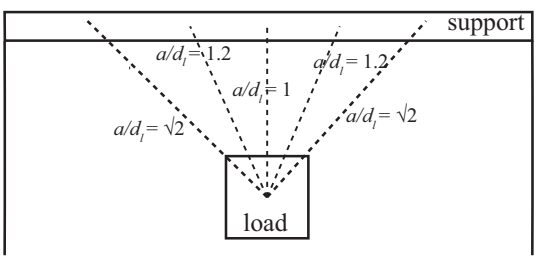

Figure 9. Larger average a/d_l ratio for slabs as compared to beams

beams, only the straight strut (a/d_l = 1 in Figure 9) can develop. In slabs, the resulting a/d_l will be influenced by the fan of struts and their average resulting load path. A larger average a/d_l results, leading to a smaller influence of the distance between the concentrated load and the support on the shear resistance of slabs. The experimental results show the difference in behaviour between the beams or slab strips with mainly two-dimensional load carrying behaviour and slabs with mainly three-dimensional load-carrying behaviour.

5 Recommendations for the effective width

*5.1 **Influence of the width***

Regan and Rezai-Jorabi [1988] suggested that the difference in shear capacity from the narrow to full width conditions as observed in experiments on slabs under concentrated loads at larger distances to the support, is the result of an interaction between the one-way and two-way shear modes. This idea is supported by the experiments from Table 3, in which the cracking patterns on the bottom face of the specimens show the differences between two-dimensional beam behaviour and three-dimensional slab behaviour. The specimens with a smaller width (BS and BM series) show a cracking pattern at the bottom face consisting mainly of straight cracks parallel to the support, Figure 10a. In the wider specimens, a more grid-like pattern with cracks perpendicular to and parallel with the span direction is visible, Figure 10b. These observations correspond to the concept of transverse load redistribution in slabs.

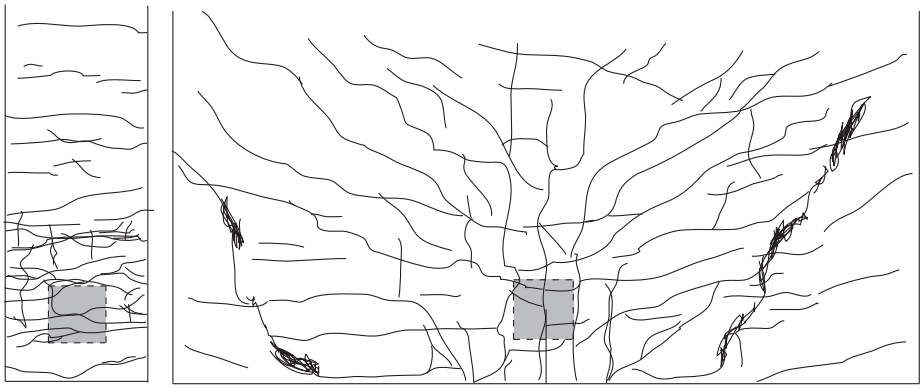

Figure 10. Difference in cracking pattern between beam and slab: (a) cracking pattern at bottom face after BS2T1, (b) cracking pattern at bottom face after S9T1. The grey area denotes the location of the loading plate. Bold lines in (b) denote areas of punching damage

For members with a smaller width, transverse load redistribution cannot occur and the load is carried directly from its point of application to the support. As seen in the previous parameter analysis, the effective width depends on the influence of the size of the loaded area, the distance between the load and the support and the moment distribution at the support. All these experimental observations can be explained based on the concept of transverse load redistribution: when the possibility of carrying load over the width direction is activated, additional loading paths develop and these paths are influenced by the geometry.

Regan and Rezai-Jorabi [1988] observed increasing maximum shear capacities for increasing widths (0.4 m to 1.2 m) up to a certain value (1 m) for a/d_l = 5.42 after which the maximum shear capacity remained around the same value. Reißen and Hegger [2012] tested slabs of increasing widths, but a threshold value cannot be observed from this series of tests. From the results of experiments on slabs under a concentrated load close to the support from the literature, only A-10-10 and B-10-10 from Table 4 can be compared. The expected increase in capacity based on the Dutch load spreading method is 2% and based on the French load spreading method is 30%. The experimental results show an increase in capacity of 25%. Thus, for this case, the French load spreading method agrees best.

The results of slabs S8 (2.5 m) and S9 (2.5 m) are compared to the results of the series of slab strips (BS1/0.5 m – BX3/2 m), all of which are made with high strength concrete (Table 2). The results are used to evaluate the horizontal load spreading methods. In line with the concept of the effective width (Figure 1), for slab strips with a small width an increase of the specimen width should lead to an increase of the shear capacity: the full specimen width carries the load at the support. For larger widths, a threshold value should apply above which no further increase in shear capacity is observed with an increasing specimen width. This threshold value corresponds to the effective width that carries the load at the support, and is –according to the concept sketched in Figure 1– independent of the specimen width. The results of the comparison of the experimental data are shown in Figure 11. These results show that the concept of using an effective width for slabs is a logical concept as the shear capacity does not increase linearly for larger widths.

The threshold effective width is determined for each of the set of parameters shown in the legend of Figure 11 by finding the intersection of the trend line through the data points for which the shear capacity is increasing with the specimen width and of the horizontal line that defines the average shear capacity which remains constant for increasing specimen

widths. The results for the calculated effective width based on the experimental results are given in Table 8 and compared to the calculated widths based on the load spreading methods from Figure 1a, b_{eff1}, Figure 1b, b_{eff2}, Figure 1c, b_{MC} and the effective width from German practice b_{DE}, the effective width from Zheng et al. [2010], b_{Zh}, and the effective width from BBK79, b_{BBK}. In Table 8, the following results are given:

b_{meas} effective width as the calculated threshold from the series of experiments with different widths;

b_{eff1} effective width based on the load spreading method as used in Dutch practice;

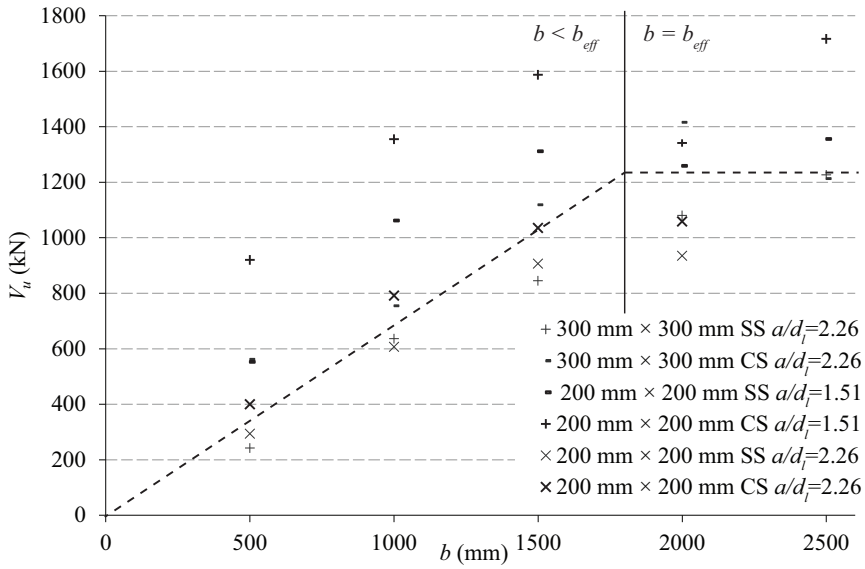

Figure 11. Influence of overall width on shear capacity. Test results for BS, BM, BL, BX, S8 and S9 are shown

Table 8. Effective width as calculated from the experimental results

Series	b_{meas} (m)	b_{eff1} (m)	b_{eff2} (m)	b_{MC} (m)	b_{DE} (m)	b_{Zh} (m)	b_{BBK} (m)
300 mm × 300 mm, SS, a/d_l = 2.26	2.04	1.1	1.7	0.99	0.87	2.79	3.21
300 mm × 300 mm, CS, a/d_l = 2.26	1.78	1.1	1.7	0.99	-	2.79	3.21
200 mm × 200 mm, SS, a/d_l = 1.51	1.31	0.7	1.1	0.63	0.67	2.71	3.08
200 mm × 200 mm, CS, a/d_l = 1.51	0.94	0.7	1.1	0.63	-	2.71	3.08
200 mm × 200 mm, SS, a/d_l = 2.26	1.53	1.1	1.5	0.98	0.77	2.71	3.08
200 mm × 200 mm, CS, a/d_l = 2.26	1.31	1.1	1.5	0.98	-	2.71	3.08

$b_{eff\,2}$ effective width based on the French load spreading method (Chauvel et al. [2007]);

b_{MC} effective width based on the load spreading method from the *fib* Model Code;

b_{DE} effective width from German practice (Grasser and Thielen [1991]), Eq. (2);

b_{Zh} effective width for bridge decks (Zheng et al. [2010]), Eq. (3);

b_{BBK} effective width from BBK 79, Eq. (4).

In Table 8, no results are given for b_{DE} at the continuous support. Grasser and Thielen [1991] recommend the use of $t_y + 0.3\,x$ for fixed-pin conditions, but only for $0.2\,l < x < l$. For the considered experiments, this would mean $a > 720$ mm. For this reason, the effective width b_{DE} is only given for experiments close to the simple support. Comparing the results of b_{meas} to the calculated effective widths in Table 8 shows that the experimental effective width corresponds best to the effective width based on the French load spreading method. The results for b_{Zh} and b_{BBK} lead to effective widths larger than the specimen width, and are not considered in further analysis for being overly unconservative. The results for b_{MC} and b_{DE} on the other hand are too conservative as compared to b_{meas} . For this reason, these results are not considered in the further analysis.

In Table 9, the results of the effective width from Eq. (1) are given (Lubell, Bentz and Collins [2008]). In this method, the effective width depends on the specimen width. Therefore, Table 9 gives the effective width for the increasing specimen sizes, both for $b_{load} = 300$ mm and $b_{load} = 200$ mm. Comparing the results of b_{meas} from Table 8 with the results in Table 9 shows that using the reduction factor β_L leads to conservative effective widths for slabs strips with $b < 2$ m (except for loading at $a/d_l = 1.51$ close to the simple support). The distance between the load and the support does not influence the effective width from Lubell, Bentz and Collins [2008]. Because this method disregards the important

Table 9. Effective width from Lubell, Bentz and Collins [2008]

b (mm)	b_{load} (mm)	κ	β_L	b_{eff} (m)	b_{load} (mm)	κ	β_L	b_{eff} (m)
500	300	0.60	0.88	0.44	200	0.40	0.82	0.41
1000	300	0.30	0.79	0.79	200	0.20	0.76	0.76
1500	300	0.20	0.76	1.14	200	0.13	0.74	1.11
2000	300	0.15	0.75	1.49	200	0.10	0.73	1.46
2500	300	0.12	0.74	1.84	200	0.08	0.72	1.81

influence of the distance between the load and the support, it is omitted from further analysis.

The results from Table 8 show a difference between loading at the simple (SS) and continuous (CS) support. Consistently, lower effective widths are found at the continuous support as compared to the simple support. This observation corresponds to the results from the linear finite element analysis, indicating the influence of the transverse moment in slabs.
The results from Table 8 also show a different effective width depending on the size of the loaded area. As previously discussed, load spreading from the centre of the load towards the support would not imply an influence of the size of the loaded area on the effective width or the overall shear capacity. The results of this series of experiments show the influence of the size of the loaded area on the effective width, as used in the French load spreading method. A larger loaded area leads to a larger effective width and thus a wider mechanism of load spreading. This observation can be explained by the larger area from which the compression struts are distributed.

Moreover, the results from Table 8 show that the effective threshold width becomes smaller as the a/d_l ratio decreases, which corresponds to the idea of horizontal load spreading from the load towards the support at a certain angle. The importance of the distance between the load and the support is reflected by both studied horizontal load spreading methods as well as the measured effective widths based on the series of slab strips. Indeed, at smaller distances between the load and the support, the compression struts cannot fan out over the width as much as at larger distances.

*5.2 **Statistical analysis***

A statistical analysis is also used to quantify which load spreading method can be recommended for use in combination with EN 1992-1-1:2005. All experiments on slabs and slab strips (Table 3, uncracked results) are analysed as well as relevant experiments from the slab shear database (Lantsoght [2012a]). Mean material properties are used, and all partial safety factors are equal to 1. The analysis shows that combining $b_{eff\,1}$ and $b_{eff\,2}$ with the shear provisions from EN 1992-1-1:2005 both lead to conservative results. The statistical analysis is shown in Table 10, with:

AVG average value;

STD standard deviation;

COV	coefficient of variation;
$V_{DUT\exp}$	the shear force at the support in the experiments from Table 3, uncracked;
$V_{EC,beff1}$	the shear capacity as prescribed by EN 1992-1-1:2005 and using b_{eff1};
$V_{EC,beff2}$	the shear capacity as prescribed by EN 1992-1-1:2005 and using b_{eff2};
V_{DUTdb}	the shear capacity as found in the experiments from the slab shear database.

The results in Table 10 show the large conservatism in the shear provisions from EN 1992-1-1:2005 when compared to the experimental results from §4.1. The 5% lower bound of the distribution of the ratio of experimental to predicted values is found to be larger than 1 for the experimental results from §4.1. The French load spreading method results in a smaller underestimation of the capacity when compared to the Delft experiments, and a significantly smaller coefficient of variation. Note that the scatter on the experiments from the slab shear database is large, as it comprises shear, punching and flexural failures (when calculating the flexural capacity for such experiments, it was found that the failure mode could have been bending, even though these failures were reported as shear failures). Moreover, the empirical equations from EN 1992-1-1:2005 take only a limited number of parameters into account. Variations in other parameters invariably lead to increases in the standard deviation. Therefore, the results of the comparison of the test results from the database with the predicted shear capacity are used here in terms of the coefficient of variation to determine the preferable load spreading method. As such, Table 10 clearly indicates that the French load spreading method leading to b_{eff2} (Figure 1b) is to be preferred.

Table 10. Comparison between EN 1992-1-1:2005 and the experimental results

	$\frac{V_{DUT\exp}}{V_{EC,beff1}}$	$\frac{V_{DUT\exp}}{V_{EC,beff2}}$	$\frac{V_{DUTdb}}{V_{EC,beff1}}$	$\frac{V_{DUTdb}}{V_{EC,beff2}}$
AVG	3.401	2.382	1.937	1.570
STD	0.890	0.522	1.228	0.659
COV	26%	22%	63%	42%

The statistical results of the comparison between the experiments and the shear capacities from EN 1992-1-1:2005 show that there is room for improvement to determine the shear capacity of slabs subjected to concentrated loads close to supports. To find better estimates for this capacity, two methods are proposed (Lantsoght, [2013]): (1) extending the formula from EN 1992-1-1:2005, based on the safety philosophy of the Eurocodes, to take the beneficial influence of transverse load redistribution further into account; and (2)

developing a mechanical model, based on the Bond Model for concentric punching shear by Alexander and Simmonds [1992]. Both resulting models (currently given in Lantsoght [2013]) are the subject of future publications.

5.3 Non-linear finite element models

Falbr [2011] and Doorgeest [2012] studied in non-linear finite element models the stress distribution at the support to assess the effective width. Doorgeest [2012] determined the effective width based on the stress distribution over the support for a series of finite element models of slabs in Diana [2012] with variable width and variable shear span, Figure 12. This analysis shows that the French load spreading method gives mostly a safe average of the effective width, although the increase of the effective width for an increasing shear span is smaller in the models than as found based on the French load spreading method. Moreover, the effective width in the models is found to be dependent on the overall slab width.

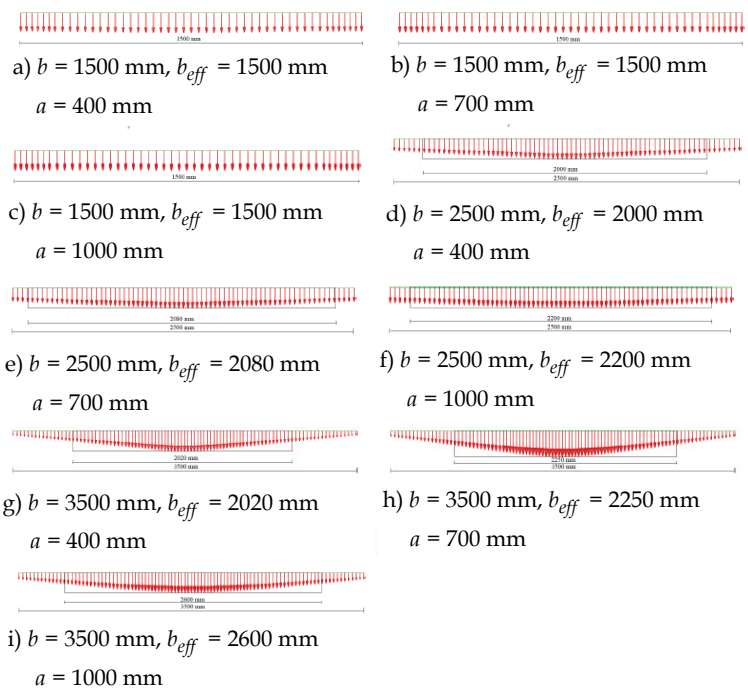

Figure 12. The vertical stress distribution in the interface layer of the support at failure, as calculated by Doorgeest [2012]

Falbr [2011] modelled the experiment S1T1 in ATENA [2011]. From this analysis, the effective width based on the shear stress distribution was found. Translating this back into a load spreading method, the required angle for load spreading from the far side of the loading plate (Alternative II) or from the centre of the loading plate (Alternative I) was defined, as shown in Figure 13. The effective width is also determined from the area over which inclined cracks at the soffit were observed in the "experiment" (the green line shows the associated load spreading method). The sketch shows a good comparison between the effective width resulting from the experimentally observed cracked region, the effective width based on the nonlinear finite element calculations and the effective width $b_{eff\,2}$ according to the French load spreading method (Alternative II in Figure 13).

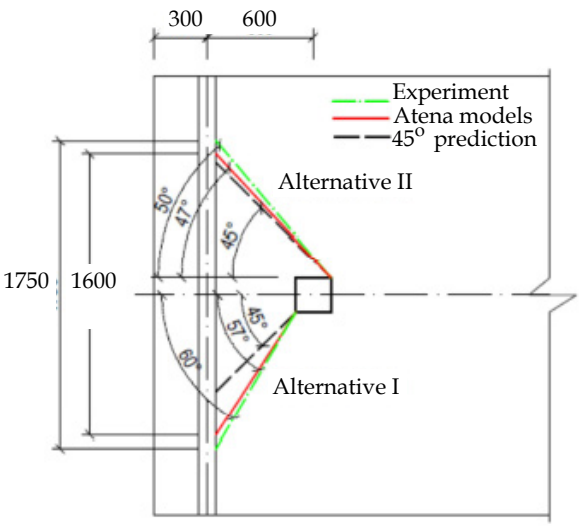

Figure 13. Comparison between different angles for the load spreading method leading to different considered effective widths: effective width based on the stress distribution over the support in Atena (red line), based on the area over which the inclined cracks on the soffit of the slab after failure in the experiment were observed (green line) and based on a load spreading method using a 45° angle (black line), calculated by Falbr [2011]. Alternative I is based on the Dutch load spreading method, while Alternative II is based on the French load spreading method.

6 Summary and Conclusions

An experimental study has been performed to assess the difference in behaviour between beams and slabs failing in shear. This difference is described in terms of the transverse load redistribution capacity that occurs in slabs as a result of their additional dimension.

An overview of the experiments reported in the literature on slabs and wide beams, failing in shear or in punching, as a result of loading with a concentrated load, multiple loads or a line load shows that only 22 shear experiments have been carried out on one-way slabs under a concentrated load close to the support. These experiments are carried out on slabs with a small depth (d_l < 150 mm).

The current research aims at studying the shear capacity of slabs under a concentrated load close to the support, for practical assessment of slab bridges in which the load model from EN 1991-2:2003 is applied and a heavy axle load is placed in the vicinity of the support. In total, 127 experiments on 18 slabs and 12 slab strips under a concentrated load close to the support have been carried out.

It can be seen from the results that when a locally failed and heavily damaged slab is tested in the vicinity of this failure, the redistribution capacity of the slab will lead to a large residual capacity (on average 81% of the capacity of an undamaged specimen).

In the experiments, it is observed that the influence of the size of the loaded area is significant, and also depends on the overall specimen width. This observation affirms that the transverse load redistribution is activated as the width of the specimen increases. For a larger loaded area, the compressive struts developing between the load and the support will have a larger base to start from. As a result, more material can be used to carry load and hence the capacity is increased.

The gradient of the support moment has a smaller influence on the shear capacity for specimens with a larger width. This influence is also observed in linear finite element analyses, explaining the role of the transverse moment in slabs for which transverse load redistribution is activated.

For slabs, it is observed that the influence of the distance between the load and the support (expressed as a/d_l) is smaller as compared to slab strips with a smaller width. Two mechanisms counteract in slabs subjected to a concentrated load closer to the support: on one hand, the struts between the load and the support become steeper, thus increasing the

capacity; on the other hand, the associated effective width in shear becomes smaller, thus decreasing the maximum shear force that can be carried. The experimental observations can be explained by imagining a fan of struts between the load and support, for which the average distance a/d_l is larger than the a/d_l distance of the straight compression strut.

The effective width in shear as used in French practice is recommended for application to slabs. This recommendation is based on the threshold values from the series of slab strips, a statistical analysis of the ratio between the experimental and predicted values based on the combination with EN 1992-1-1:2005 and the studied load spreading methods for the effective width, and non-linear finite element models. The non-linear finite element models show that, while using the French load spreading method leads to reliable results; it does not cover all parameters that were found to affect the stress distribution and effective width at the support. It is thus shown that the shear capacity of slabs under a concentrated load close to the support can be calculated by using the shear capacity from EN 1992-1-1:2005 over the recommended effective width.

Overall, the experiments, parameter analysis and comparison to the shear capacity from EN 1992-1-1:2005 show that slabs subjected to a concentrated load close to the support fail in a three-dimensional shear mode that is distinctly different from the two-dimensional failure mode of beams.

Acknowledgement

The authors wish to express their gratitude and sincere appreciation to the Dutch Ministry of Infrastructure and the Environment (Rijkswaterstaat) for financing this research work and InfraQuest for coordinating the cooperation between Delft University of Technology, Rijkswaterstaat and the research institute TNO.

Literature

Alexander, S.D.B. and Simmonds S.H. (1992), Bond Model for Concentric Punching Shear, *ACI Structural Journal*. 89: 325-334.

ATENA. ATENA Program Documentation Part 2-2: User's Manual for ATENA 3D Version 4.3.0, 2011.

Azad, A. K., Baluch, M. H., Almandil, M. Y., Sharif, A. M. and Kareem, K. (1993). Loss of punching capacity of bridge deck slabs from crack damage. *ACI Structural Journal*. 90: 37-41.

BBK. Regulations for concrete structures - Part 1: Design. Statens Betong Kommitte. Stockholm. 1979.

CEN. Eurocode 1: Actions on structures - Part 2: Traffic loads on bridges, EN 1991:2-2003. 2003.

CEN. Eurocode 2 – Design of Concrete Structures: Part 1-1 General Rules and Rules for Buildings. EN 1992-1-1:2005. 2005.

Chauvel, D., Thonier, H., Coin, A. and Ile, N. Shear Resistance of slabs not provided with shear reinforcement CEN/TC 250/SC 02 N 726. 2007.

Clark, A. P. (1951). Diagonal Tension in Reinforced Concrete Beams. *ACI Journal Proceedings*. 48: 145-156.

Code Committee 351001 (Code Committee 351001). NEN 6720 Technical Foundations for Building Codes, Concrete provisions TGB 1990 - Constructive requirements and calculation methods (VBC 1995). 1995. (in Dutch)

Doorgeest, J. Transition between one-way shear and punching shear. MSc Thesis Delft University of Technology. 2012.

Ekeberg, P. K., Sjursen, A. and Thorenfeldt, E. (1982). Load-carrying capacity of continuous concrete slabs with concentrated loads. Nordisk betong. 4: 153-156. (in Norwegian)

Falbr, J. Shear redistribution in solid concrete slabs. MSc Thesis Delft University of Technology. 2011.

fib. Model Code 2010: Final Draft. Lausanne, International Federation for Structural Concrete. 2012.

Furuuchi, H., Takahashi, Y., Ueda, T. and Kakuta, Y. (1998). Effective width for shear failure of RC deep slabs. *Transactions of the Japan concrete institute*. 20: 209-216.

Graf, O. (1933). Experiments on the Capacity of Reinforced Concrete Slabs under Concentrated Loads close to a Support. Deutscher Ausschuss für Eisenbeton. 73: 10-16. (in German)

Grasser, E. and Thielen G. (1991). Design aid for the calculation of sectional forces and deformations of reinforced concrete structures. Deutscher Ausschuss für Stahlbeton, 240: 1-86. (in German)

Hamadi, Y. D. and Regan, P. E. (1980). Behaviour in shear of beams with flexural cracks. *Magazine of Concrete Research*. 32: 67-78.

Hofbeck, J. A., Ibrahim, I. O. and Mattock, A. H. (1969). Shear Transfer in Reinforced Concrete. *ACI Journal Proceedings*. 66: 119-128.

Kani, G. N. J. (1964). The Riddle of Shear Failure and Its Solution. *ACI Journal Proceedings*. 61: 441-467.

Lantsoght, E. O. L. Shear tests of reinforced concrete slabs: experimental data of residual capacity of slabs. Stevinrapport nr 25.5-11-08: Delft University of Technology, the Netherlands. 2011a.

Lantsoght, E. O. L. Shear tests of reinforced concrete slabs: experimental data of undamaged slabs. Stevinrapport nr 25.5-11-07: Delft University of Technology, The Netherlands. 2011b.

Lantsoght, E. O. L. Shear in reinforced concrete slabs under concentrated loads close to the support – Literature review. Stevinrapport 25.5-12-11: Delft University of Technology. 2012a.

Lantsoght, E. O. L. Shear tests of reinforced concrete slabs and slab strips under concentrated loads. *Proceedings of The 9th fib International PhD Symposium in Civil Engineering*. Karlsruhe Institute of Technology (KIT), 22 – 25 July 2012, Karlsruhe, Germany: 3-8, 2012b.

Lantsoght, E. O. L. Progress report: Experiments on slabs in reinforced concrete: Part II: analysis of the results. Stevinrapport 25.5-12-10: Delft University of Technology, the Netherlands. 2012c. (in Dutch)

Lantsoght, E. O. L., van der Veen, C. and Walraven, J. C. Shear assessment of solid slab bridges. ICCRRR 2012, *3rd International Conference on Concrete Repair, Rehabilitation and Retrofitting*. Cape Town, South Africa: 827-833, 2012a.

Lantsoght, E. O. L., van der Veen, C. and Walraven, J. C. (2012b). Shear capacity of slabs and slab strips loaded close to the support. ACI SP-287, Recent Development in Reinforced Concrete Slab Analysis, Design and Serviceability. 5.1-5.18.

Lantsoght, E.O.L. *Shear in Reinforced Concrete Slabs under Concentrated Loads Close to Supports*. PhD Thesis: Delft University of Technology, the Netherlands. 2013.

Lantsoght, E. O. L., van der Veen, C. and Walraven, J. C. (2013). Shear in One-way Slabs under a Concentrated Load close to the support. *ACI Structural Journal*. 110: 275-284.

Leonhardt, F. and Walther, R. (1962). Contributions to the Treatment of the Shear Problem in Reinforced Concrete - 2. Continuation of Chapter II. Experimental report. *Beton- und Stahlbetonbau*. 57: 54-64. (in German)

Lubell, A.S., Bentz E., and Collins M.P. (2008). One-Way Shear in Wide Concrete Beams with Narrow Support. ASCE Structures Congress, Vancouver, Canada.

Prochazkova, Z. and Lantsoght, E. O. L. Material properties – Felt and Reinforcement For Shear test of Reinforced Concrete Slab. Delft University of Technology. 2011.

Rafla, K. (1971). Empirical Formulas for the Calculation of the Shear Capacity of Reinforced Concrete Beams. *Strasse Brucke Tunnel*. 23: 311-320. (in German)

Regan, P. E. Shear Resistance of Concrete Slabs at Concentrated Loads close to Supports. Polytechnic of Central London. 1982.

Regan, P.E., Shear Resistance of Members without Shear Reinforcement; Proposal for CEB Model Code MC90. Polytechnic of Central London. 1987.

Regan, P. E. Enhancement of shear resistance in short shear spans of reinforced concrete - an evaluation of UK reccomendations and particularly of BD44/95. University of Westminster. 1998.

Regan, P. E. and Rezai-Jorabi, H. (1988). Shear Resistance of One-Way Slabs under Concentrated Loads. *ACI Structural Journal*. 85: 150-157.

Reißen, K. and Hegger, J. Shear Capacity of Reinforced Concrete Slabs under Concentrated Loads. IABSE 2012. Seoul, South Korea. 2012.

Richart, F. E. An investigation of web stresses in reinforced concrete beams, bulletin No. 166 of the Engineering Experiment Station. 24: University of Illinois. 1927.

Richart, F. E. and Kluge, R. W. Tests of reinforced concrete slabs subjected to concentrated loads; a report of an investigation. 36: University of Illinois. 1939.

Sherwood, E. G., Lubell, A. S., Bentz, E. C. and Collins, M. R. (2006). One-way shear strength of thick slabs and wide beams. *ACI Structural Journal*. 103: 794-802.

Talbot, A. N. Tests of reinforced concrete beams: resistance to web stresses, bulletin No. 29 of the Engineering Experiment Station. 6: University of Illinois. 1909.

TNO DIANA. User's Manual of DIANA, Release 9.4.4, Delft, the Netherlands. 2012.

Yang, Y. Report of Experimental Research on Shear Capacity of Beams Close to Intermediate Supports. Stevinrapport 25.5-11-10: Delft University of Technology, the Netherlands. 2011.

Zheng, Y., Taylor, S., Robinson, D. and Cleland, D. (2010). Investigation of Ultimate Strength of Deck Slabs in Steel-Concrete Bridges. *ACI Structural Journal*. 107: 82-91.